World Academy of Science, Engineering and Technology
International Journal of Physical and Mathematical Sciences
Vol:9, No:7, 2015

Numerical Simulation of Fluid-Structure Interaction on Wedge Slamming Impact Using Particle Method

Sung-Chul Hwang, Di Ren, Sang-Moon Yoon, Jong-Chun Park, Abbas Khayyer, Hitoshi Gotoh

***Abstract*—**This paper presents a fully Lagrangian coupled Fluid-Structure Interaction (FSI) solver for simulations of fluid-structure interactions, which is based on the Moving Particle Semi-implicit (MPS) method to solve the governing equations corresponding to incompressible flows as well as elastic structures. The developed solver is verified by reproducing the high velocity impact loads of deformable thin wedges with three different materials such as mild steel, aluminium and tin during water entry. The present simulation results for aluminium are compared with analytical solution derived from the hydrodynamic Wagner model and linear Wan's theory. And also, the impact pressure and strain on the water entry wedge with three different materials, such as mild steel, aluminium and tin, are simulated and the effects of hydro-elasticity are discussed.

***Keywords*—**Fluid-structure interaction (FSI), Moving Particle Semi-implicit (MPS) method, Elastic structure, Incompressible fluid Wedge slamming impact.

I. Introduction

WEDGE slamming impact problem has always been widespread concerned in various engineering fields, such as seaplane landing, recycling for the satellite re-entry capsule, or the impact load of the bow in the adverse sea conditions so on, and also always plays the significant role on the structural safety. Due to its strong nonlinearity, however, it seems to be not easy to find the exact solution or obtain the accurate simulation results to predict the impact loads on water entry. Furthermore, combined with the strong interaction between the fluid and elastic structure, so-called fluid-structure interaction (FSI), the enhanced difficulty for numerical simulation leads to a new level for challenging [1], [2].

This paper covers the FSI simulation on a wedge slamming probelm using a fully Lagrangian coupled FSI solver [5] corresponding to incompressible fluid flows and elastic structures based on Navier-Stoeks and continuity equations for the fluid, and linear and angular momentum conservation equations for the elastic structure. The particle interaction modelling in the solver is based on the Moving Particle Semi-implicit (MPS) method [3] and PNU-MPS method [4] modified by Pusan National University, and the interface coupling between two media is performed in the same manner as a previously developed FSI solver [5] by the authors.

In this paper, firstly the developed FSI solver is validated for predicting the high velocity impact loads of deformable thin wedge with aluminium material during water entry through the comparison with an analytic solution derived from the hydrodynamic Wagner model and linear Wan's theory [6], [7]. And then the impact pressure and strain on the water entry wedge with three different materials, such as mild steel, aluminium and tin, are simulated and the effects of hydro-elasticity are discussed.

S.-C. Hwang is with the Korea Research Institute of Ships and Ocean Engineering, Daejeon, Republic of Korea (e-mail: schwang@kriso.re.kr).

D. Ren and S.-M. Yun are with the Department of Naval Architecture and Ocean Engineering, Pusan National University, Busan, Republic of Korea (e-mail: rendi3077@pnu.edu, ymrb2804@pnu.edu).

J.-C. Park is with the Department of Naval Architecture and Ocean Engineering, Pusan National University, Busan, Republic of Korea (corresponding author to provide phone: +82-51-510-3106; fax: +82-51-512-8836; e-mail: jcpark@pnu.edu).

A. Khayyer and H. Gotoh are with the Department of Civil and Earth Resources Engineering, Kyoto University, Kyoto, Japan (e-mail: khayyer@particle.kuciv.kyoto-u.ac.jp, gotoh@particle.kuciv.kyoto-u.ac.jp).

II. Numerical Method

For the governing equation in the developed FSI solver, the momentum conservation equation is considered as:

$$\left(\frac{D\vec{u}}{Dt}\right)=\frac{1}{\rho}\nabla\cdot\sigma_{ij}+\vec{F}_C \tag{1}$$

where, $\vec{u}$, ρ, t represent the velocity vector, density and time, respectively. Here $\vec{F}_C$ denotes the coupling force at the interface between two phases. The stress tensor σ_{ij} can be defined in (2) and (3) for the fluid and structure phases, respectively as:

$$\sigma_{ij,F}=-p\delta_{ij}+\mu_F\frac{1}{2}\left(\frac{\partial u_i}{\partial x_j}+\frac{\partial u_j}{\partial x_i}\right) \tag{2}$$

$$\sigma_{ij,S}=\lambda_S\frac{\partial u_k}{\partial x_k}\delta_{ij}+\mu_S\frac{1}{2}\left(\frac{\partial u_i}{\partial x_j}+\frac{\partial u_j}{\partial x_i}\right) \tag{3}$$

where, p, δ, μ_F imply the pressure, Kronecker's delta, dynamic viscosity of fluid, respectively. In (3), λ_S and μ_S are the Lame's constants corresponding to material properties of structure defined as:

$$\lambda_S=\frac{E_S\nu_S}{(1+\nu_S)(1-2\nu_S)} \tag{4}$$

$$\mu_S=\frac{E_S}{2(1+\nu_S)} \tag{5}$$

Here, E_S and ν_S indicate the Young's modulus and Poisson ratio, respectively.

For the fluid phase, the continuity equation is considered for

satisfying the incompressibility as:

$$\frac{D\rho}{Dt} = 0 \tag{6}$$

For the structure analysis, furthermore, the angular momentum conservation equation is considered as:

$$\frac{D(I\vec{\omega})}{Dt} = \frac{D(\vec{r} \times m\vec{u})}{Dt} \tag{7}$$

where, I, $\vec{\omega}$, $_m$, $\vec{r}$ denote momentum of inertia, angular velocity vector, mass and location vector of a local particle, respectively.

Fig. 1 shows the solution procedure of the FSI coupled algorithm, and the details are described in [5].

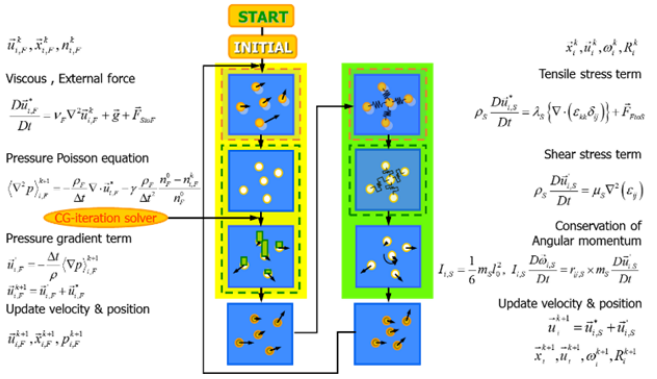

Fig. 1 The solution procedure of FSI coupled algorithm

III. Simulation Condition

The FSI simulation is implemented by a wedge with flexible plate. The center and both sides of the plate are fixed, as shown in Fig. 2. The time step is set at 0.000001s, the particle size by 0.0025m and total number of particles used is about 2163780. The location of pressure and strain monitoring points is illustrated in Fig. 3.

To compare the different effects of three different metal materials produced in the fluid-structure coupling simulation, we ran 3 cases with material properties of aluminium, Mild steel and tin. And the material properties are summarized in Table I.

TABLE I
MATERIAL PROPERTIES

Properties	Case A Aluminium (Al)	Case B Mild Steel (Fe)	Case C Tin (Sn)
Young's modulus	67.5 GPa	210 GPa	50 GPa
Poisson ratio	0.34	0.303	0.36
Density	2700 kg/m^3	7850 kg/m^3	5769 kg/m^3

IV. Simulation Results and Analysis

To validate our simulation, the time history of pressure results in case A were compared with an analytic solution. The analytical solution was calculated by the hydrodynamic Wagner model and linear Wan's theory [6] by [7]. According to the boundary conditions of the analytic solution, at the both ends of the bottom plate and the vertex point of wedge deformations and rotations were not allowable.

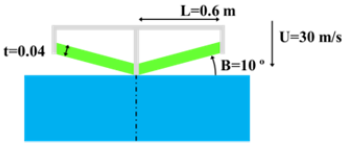

Fig. 2 Initial condition of the wedge

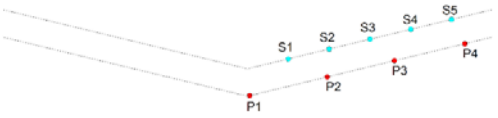

Fig. 3 Location of monitoring points

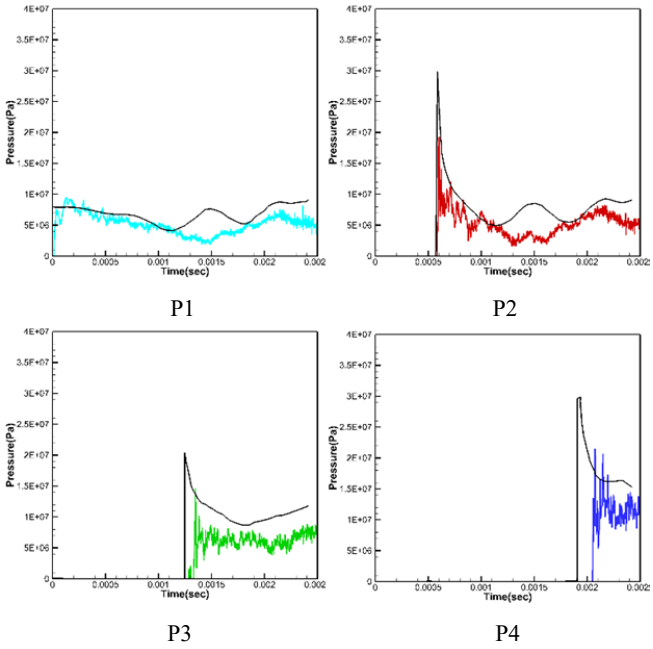

Fig. 4 Time history of pressure for case A compared with analytic solution

The verification of results was shown in Fig. 4. For the first two monitoring points, it shows a good match. But for the other two monitoring points, the delay is obvious. And the time history of pressure for case B and case C was shown in Figs. 5 and 6.

Fig. 7 shows the snapshots of the simulation results in 0.0004 second and 0.0020 second. The colour of fluid particles shows the pressure, the colour of structure particles shows the stress, and the black solid line shows the contour of zero stress. The deformation cause by pressure is obviously in the snapshots. And it shows that the water pile-up and jet were well simulated by present method. The solid line shows that at 0.0004s the composition of the third mode is visible only in case A and case C, not for case B.

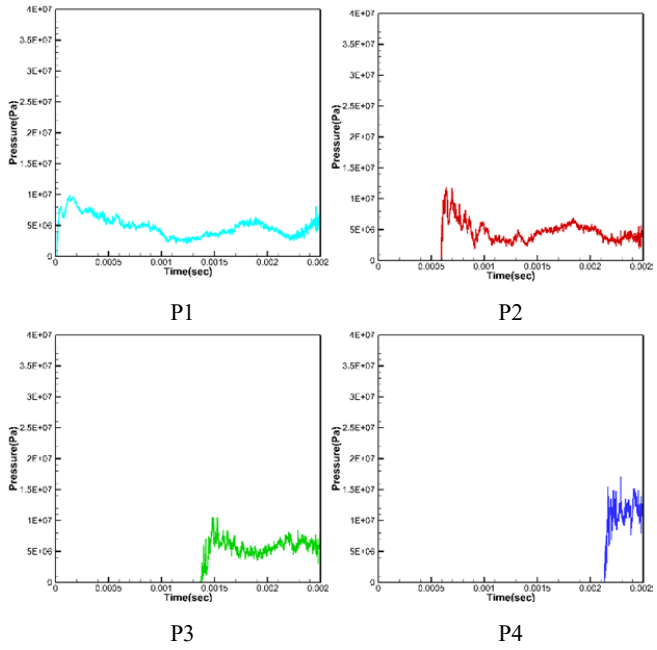

Fig. 5 Time history of pressure for case B

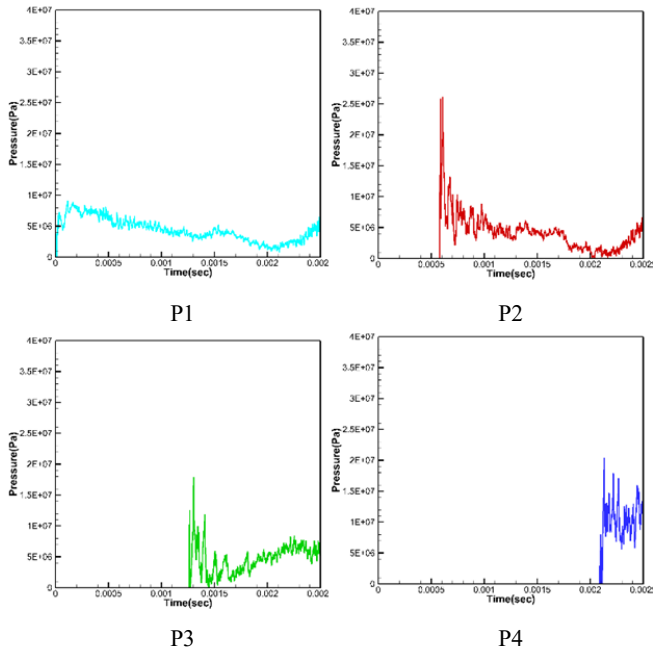

Fig. 6 Time history of pressure for case C

Fig. 8 shows the time history of strain in case A. Because of the fixed boundary condition, the two monitoring points near the boundary shows an opposite behaviour with the other points. For the other monitoring points, the sequence they increased is as same as the sequence when the peak value of pressure moved through their location. And finally, after the peak value go through the end of the wedge, the centre monitoring point (S3) got the maximum value.

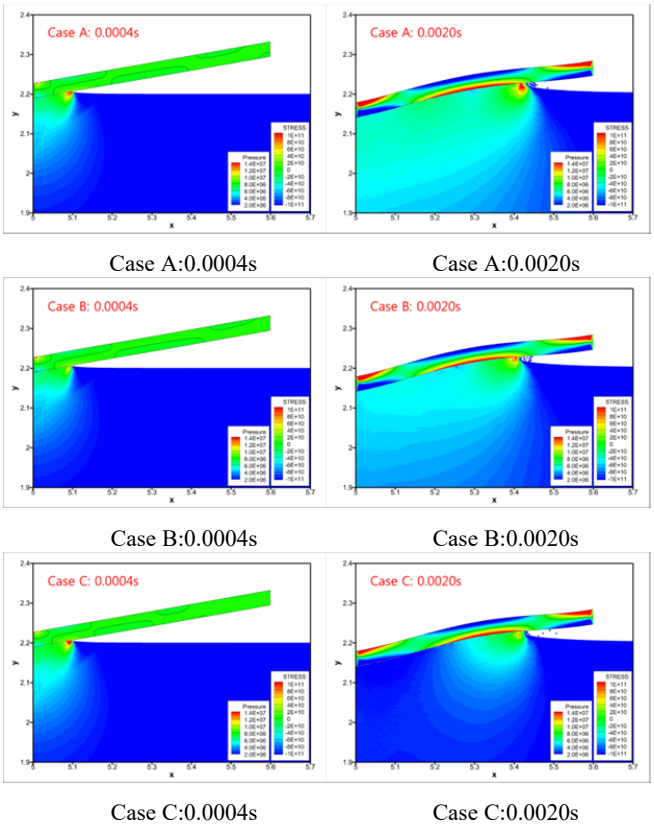

Fig. 7 Snapshots of FSI behavior for 3 cases at 0.0004 and 0.0020 second

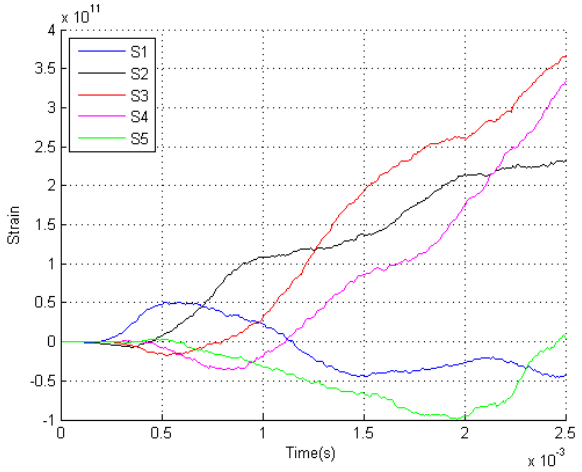

Fig. 8 Time history of strain at S1~S5 in case A

Fig. 9 shows the time history of strain at S1~S5 in case B. Unlike case A, after the peak value go through the end of the wedge, the value at monitoring points S3 and S4 are almost same.

Fig. 10 shows the time history of strain at S1~S5 in case C. Similar to case B, after the peak value go through the end of the wedge, the value at monitoring points S3 and S4 are almost same. But the curve shows more tortuous than case B.

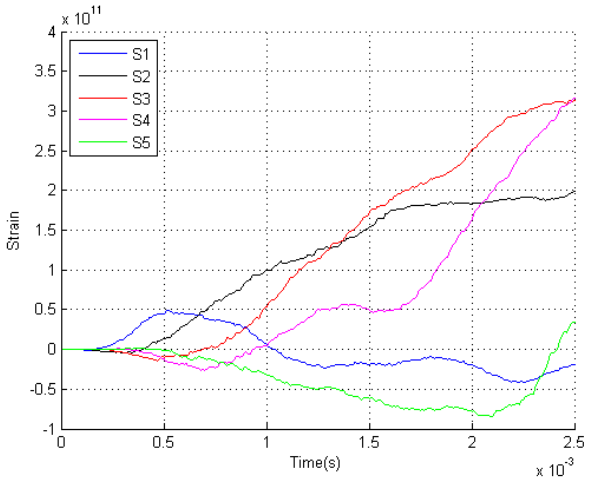

Fig. 9 Time history of strain at S1~S5 in case B

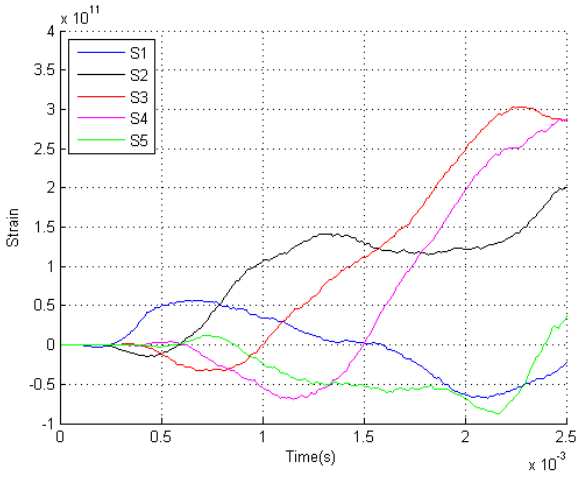

Fig. 10 Time history of strain at S1~S5 in case C

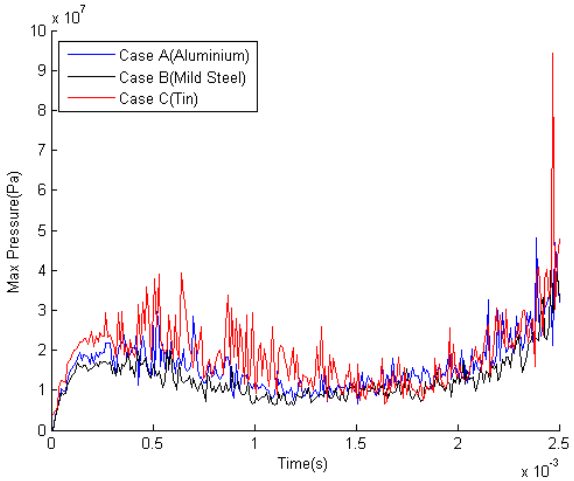

Fig. 11 Time history of max pressure for 3 cases

V. Discussion

In order to understand the effect of the different vibration mode, we drew the time history of max pressure for the 3 cases. It was shown in Fig. 11. Although it is hard to define it in the latter half part, but in the earlier half part it is clear that the max pressure of case C is higher than case B and higher than case A. Since case C has the smallest stiffness, so we can speculate that the different vibration mode caused the higher max pressure.

To compare the load conditions between 3 cases, we calculated the pressure integration on the wet surface of the wedge. And the time histories of force for 3 cases have shown in Fig. 12. Although the time histories of force is different between different cases, but when the peak value of pressure reached the end of the wedge, the force acting on the wet surface is almost same between different cases.

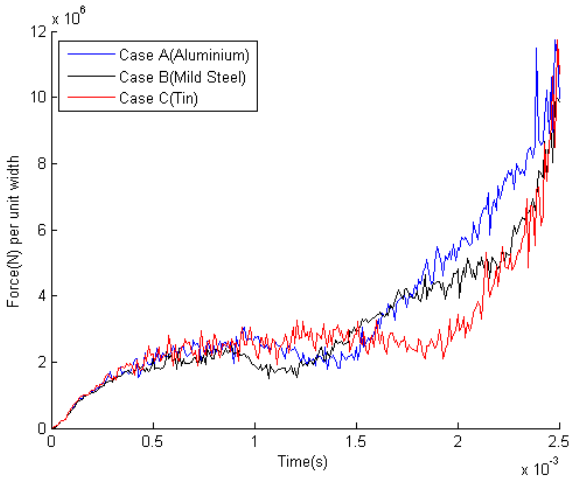

Fig. 12 Time history of force for 3 cases

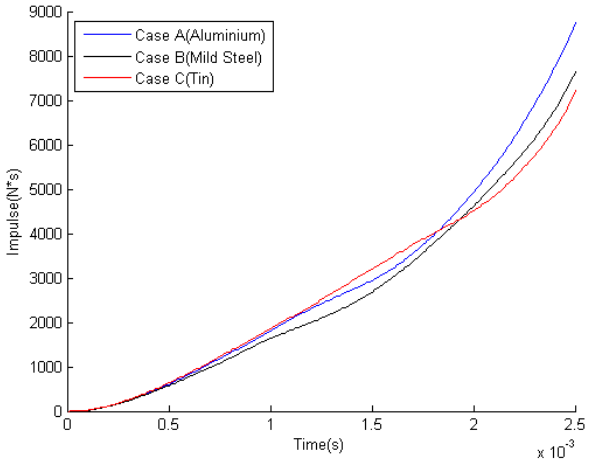

Fig. 13 Time history of impulse for 3 cases

By integrated the force acting on the wet surface over time, we get the time history of impulse for 3 cases. And the results have shown in Fig. 13. It shows that case A (the aluminium case) got the max impulse value when the peak pressure value reached the end of the wedge. Since the stiffness of aluminium is in between mild steel and tin, so the impulse in FSI problem can't be considered easily by the linear ways. And that is why we need particle method for FSI problem.

VI. Conclusion

For forced falling problem, case C shows more high-order vibration mode than case A and case B.

For low stiffness structure case, the high-order vibration mode could cause a higher pressure than the high stiffness structure case. Because of that, we need these kinds of particle method to measure the slamming load for these kinds of problems.

When the peak value of pressure reaches the end of the wedge, the total fluid force is almost same in the 3 cases.

When the end of wedge entered water, case A (the aluminium case) got the max impulse during the wedge dropping into water. Since the stiffness of aluminium is in between mild steel and tin, so the impulse in FSI problem can't be considered easily by the linear ways. And that is why we need particle method for FSI problem.

Acknowledgment

This work was supported by the Technology Innovation Program, No.10051136, funded by the Ministry Trade, Industry & Energy, Republic of Korea.

References

[1] G. Oger, L. Brasset, P. M. Guilcher, E. Jacquin, J. B. Deuff, and D. Le Touze, "Simulation of hydro-elastic impacts using a parallel SPH model," *Proceeding of ISOPE,* 2009, pp. 316-324.

[2] Y. Yamada, T. Takami, and M. Oka, "Numerical Study on the Slamming Impact of Wedge Shaped Obstacles considering Fluid- Structure Interaction (FSI)," *International Offshore and Polar Engineering Conference,* Rhodes, Greece, 2012, pp.1008-1016.

[3] S. Koshizuka, and T. Oka, "Moving-particle semi-implicit method for fragmentation of incompressible fluid," *Nuclear Sci. and Engr.*, vol. 123, no. 3, 1996, pp. 421-434.

[4] B. H. Lee, J. C. Park, M. H. Kim, and S. C. Hwang, "Step-by-step improvement of MPS method in simulating violent free-surface motions and impact loads," *Comput. Methods Appl. Mech. Engrg.*, vol. 200, no. 9, 2011, pp. 1113-1125.

[5] S. C. Hwang, A. Khayyer, H. Gotoh, and J. C. Park, "Development of a fully Lagrangian MPS-based coupled method for simulation of fluid–structure interaction problems," *Journal of Fluids and Structures,* 2014, vol. 50, pp. 497-511.

[6] F. Y. Wan, "On the equations of the linear theory of elastic conical shells," *Stud. Appl. Math,* vol. 49, no. 1, 1970, pp. 69-83.

[7] Y. M. Scolan, "Hydroelastic behavior of a conical shell impacting on a quiescent-free surface of an incompressible liquid," *Journal of Sound and Vibration*, vol. 277, 2004, pp. 163-203.